LARGE-SCALE TESTS OF FLAME SPREAD ON ROOF BUILD-UPS WITH PV SYSTEMS: PHASE I

11/2025

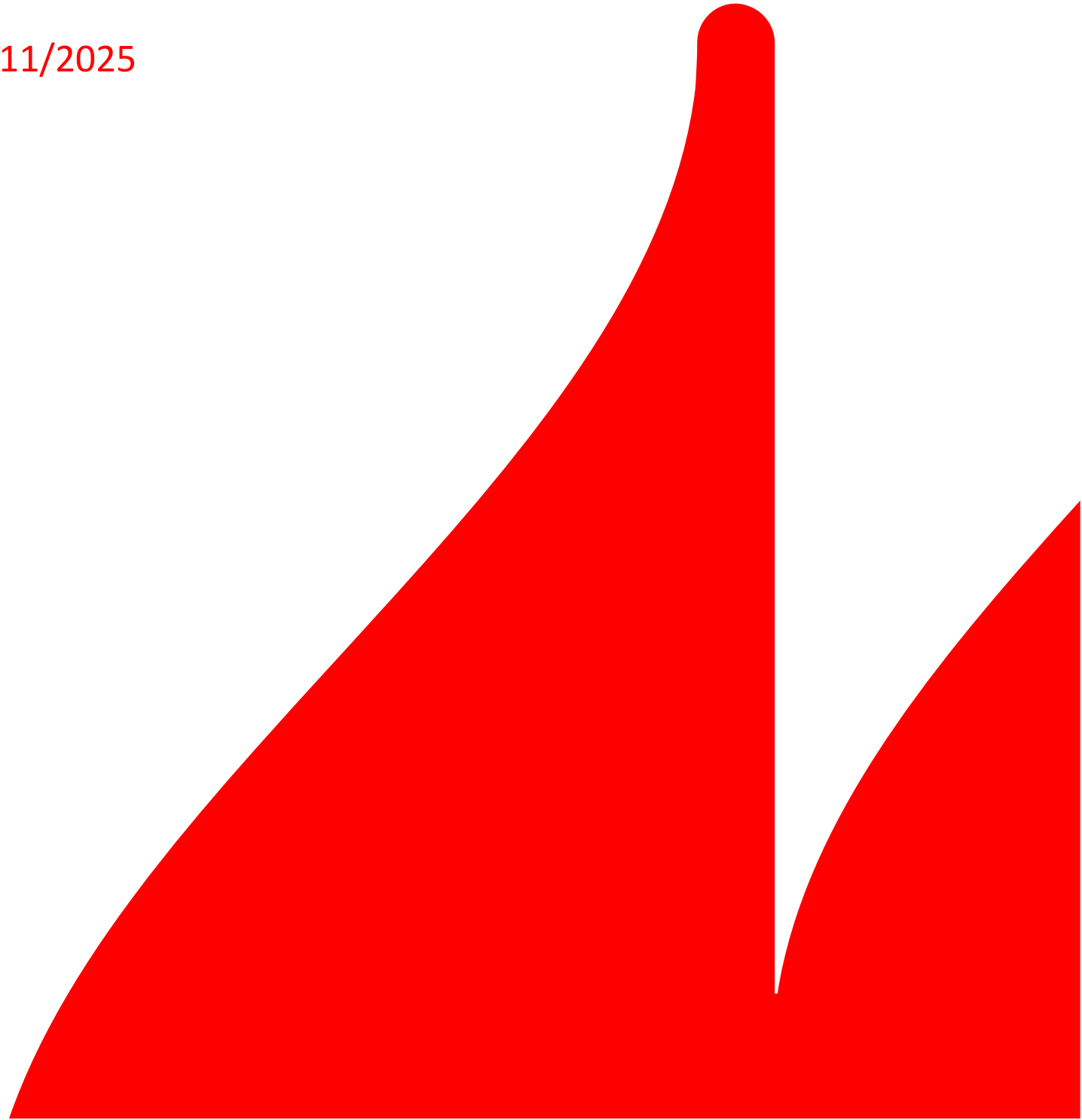

REPORT INFORMATION

Client:	EUMEPS – European Manufacturers of Expanded Polystyrene	
Address:	71 Avenue Cortenbergh B-1000 1000 Brussels Belgium	
Case number:	SIEC21006	
Report number:	21006-001	
Prepared by:	M. Sturdy, M.Sc	msu@dbigroup.dk
Revised by:	J. Steemann Kristensen, PhD	jsk@dbigroup.dk
Approved by:	A. Frost-Jensen, Director of Infrastructure & Quality	afj@dbigroup.dk

Document revision history:			
Revision number	**Date**	**Pages**	**Change description**
0	2025-08-27	All	
1	2025-10-29	All	"Cement fiber board (CFB)" changed to "cement-bonded particle board (CPB)"
2	2025-11-27	All	Final version based on comments from Steffen Kahrmann.

INTRODUCTION

In this report the Danish Institute for Fire and Security Technology (DBI) outlines the method and results of four large-scale tests conducted by IVH, the German Rigid Foam Industry Association and EUMEPS, the European Manufacturers of Expanded Polystyrene. In these tests, the performance of four different roof constructions was assessed, when a fire was initiated in the cavity between the roof surface and an array of four building applied photovoltaic (BAPV) modules.

As part of the European Union's Energy Performance of Buildings Directive, photovoltaic (PV) systems are required on an increased amount of the built environment [1]. However, the implementation of the technology introduces an increased fire-related risk as outlined by several stakeholders, including Swiss RE [2] and recently conducted research [3], [4].The fire-related risk of BAPV systems arises from an increased probability of ignition and altered fire dynamics within the cavity between the roof surface and the backside of the BAPV module.

Analysis of four different tests performed at the premises of Twente Safety Campus (Troned, NL) are presented in this report. The focal point of the four tests was to determine and compare the outcome of a PV-related fire on each of the four different roof build-ups. Two roof build-ups simulate newly built roof-structures and two simulate existing roofs retrofitted with an additional layer of insulation and building applied PV system. The design of the roof build-ups and their construction were determined by IVH and EUMEPS and assembled two days prior to the test days, October 30th, 2024, and January 29th 2025. DBI provided feedback related to the test design and instrumentation of the roof build-ups as well as attended and observed the four tests. KIWA conducted the testing and provided four test reports [5], [6], [7], [8] to IVH and EUMEPS, who shared the reports, videos, and thermocouple data with DBI. Based on that, DBI analysed the results which are presented in this report.

No significant differences were observed between the newbuilt and retrofitted roof build-ups and thus, the qualitative analysis of the tests are based on three variables: i) the type of roofing membrane, ii) type of mitigation layer and iii) ambient conditions.

The report is structured as follows: First, the four roof configurations are presented along with their respective characteristics. This is followed by a description of the instrumentation setup, a visual analysis of the fire behaviour, and a presentation of the relevant temperature measurements. The results are discussed through the report, which concludes with a brief summary discussing the influence of the various parameters investigated.

Figure 1 - Aerial view of test 1 and test 2 (closest) in October 2024 at the test area.

TEST SETUPS

This section outlines the different tests performed and presents the description of the test setups and their location. The test location, test built-up and instrumentation is presented in the following part of the report.

1.1. Location of tests

Prior to each test day, two test setups were constructed in a designated test area located between several buildings, as shown in Figure 1 and Figure 2. The surrounding building, primarily situated to the east and west of the test site, provided some shielding from potential wind effects. The tests were conducted sequentially, one at a time.

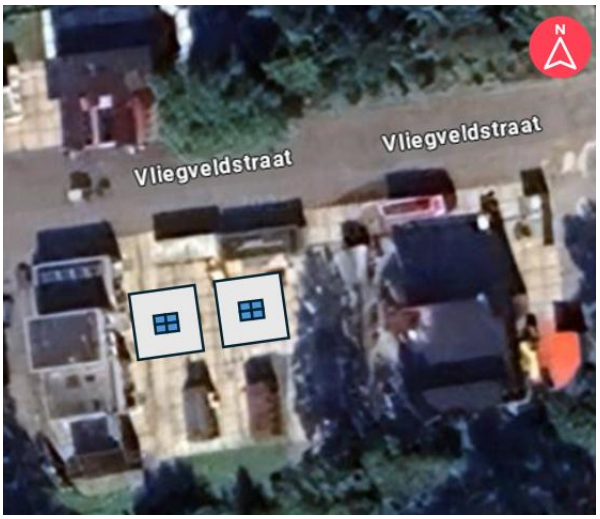

Figure 2 – Test location and construction orientation. The picture in Figure 1was taken from the roof of the ceiling of the buildings to the left (west) of the two test set-ups.

All four tests were conducted using an array of four PV modules mounted on an aluminium support structure installed above the roof. The mounting system was configured for an East/West orientation, as illustrated in Figure 1. This configuration was preferred because it allows the PV modules to be installed closer to the roof surface compared to systems designed for south-facing orientation. Previous research has shown that a reduced gap height between the underside of the PV modules and the roof surface results in a more severe flame spread scenario [9]

1.2. Roof build-ups

In all tests, the roof build-ups covered an area of 49 m², with side lengths of 7 meters. They were constructed atop a metal support structure and a 0.75 mm thick trapezoidal steel deck, identified as layers 1 and 2 in Figure 3 and Table 1.

In tests 1 and 2, two layers of 110 mm thick expanded polystyrene (EPS) insulation containing a polymeric fire retardant were installed in the roof assemblies. This build-up reflects insulation standards typical of newly built modern commercial warehouses. Tests 3 and 4 represented existing roof build-ups that were initially insulated with 80 mm EPS insulation below a bitumen roof covering (layers 3 and 4 in Table 1), retrofitted with an additional layer of 180 mm EPS and a new layer of roof covering. In all tests, the EPS insulation was classified Class E in accordance with EN 13501-1.

As outlined in Table 1, there were three key differences among the four tests: (i) the type of roofing membrane used in Layer 7, (ii) the choice of mitigation barrier in Layer 6, and (iII) the applied wind load. The use of both a 1.8 mm thick Bauder Thermofol M18 (B_{ROOF}(t1)) PVC membrane and 8 mm dual layer Bitumen-based roofing membrane (both B_{ROOF}(t1)) could be employed to test how two different products available on the market affected the same subjacent roof built-up, whereas the two different mitigation materials (layer 6) in tests 1 and 2 was tested with the purpose of evaluating the performance of the glass-fleece (GF) and of the cement-bonded particle board (CPB) in mitigating the consequences of a PV-related fire. Based on the outcome of tests 1 and 2, the effect of the CPB was examined further in tests 3 and 4, which were both based on an existing roof construction built in accordance with layers 1 to 7 in Table 1.

In tests 3 and 4 the eastern edge of each roof build-up was elevated 14 cm above the western edge, resulting in a 2° roof inclination. This inclination aligns with the minimum slope requirements specified in most European

building regulations. Based on fundamental flame spread theory, the inclination renders the flame spread in the direction towards east slightly more concurrent than towards west. Under controlled laboratory conditions, the inclination could affect the outcome of the tests. However, the influence of the cavity between the PV modules and roof surface, as well as the wind load are expected to have a more significant influence on the outcome of the tests than the inclination of the roofs build-ups and for that reason, the inclination is not discussed further in the report.

Mass and specific heat were the main differences between the two types of mitigation layers, as the mass of the cement-bonded particle board was significantly higher than that of the glass-fleece as shown in Table 2. The specific heat capacity differed slightly between the two materials, with partially higher values for the fleece which requires greater energy to change its temperature. Between the two properties, in this case the considerable difference in mass is more prevalent.

Comparing the roof constructions for tests 2 and 3, one can see how the composition of Layers 6-7 remain identical. While similar in build-up characteristics, the differences in external conditions between test 2 and test 3 highlighted in Table 2 lead to significant differences in the results of the tests: discussion of these differences is undertaken in the following sections. In test 4, utilization of Bitumen as the roof membrane instead of PVC in Layer 8 was investigated. Furthermore, since test 4 was performed on the same day as test 3, the effect of moderate wind on the test outcome was also investigated. Comparison in performance of the two different retrofitting constructions from tests 3 and 4 is also discussed in Chapter 2.

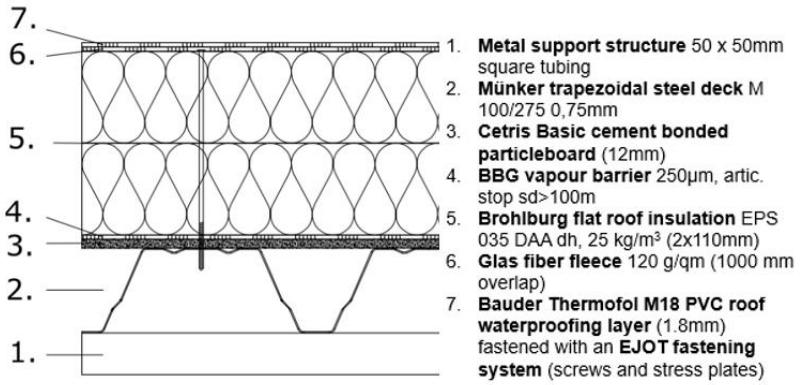

Figure 3 - Detail of the roof construction layers from Test 1.

Salient characteristics of the different materials utilized in tests 1- 4 are presented in Table 1 below. References to the material properties presented in Table 2 is made in later sections of the report.

Table 1 - Test matrix of the four conducted tests, presented as layers and ambient wind speed. Materials in each layer corresponds in Figure 3. In tests 3 and 4, the vapour barrier below the EPS insulation in layer 4 is omitted. The numbered red dots mark the location of the thermocouple groups described in subsection 1.5.
** CPB: Cement-bonded particle Board.*

Layer	Test 1	Test 2	Test 3	Test 4
# 7	1.8 mm PVC-based roofing membrane ③		③	8 mm Bitumen ③
# 6	1.2 mm Glass Fleece ③	12 mm CPB* ②	②	②
# 5	220 mm EPS		180 mm EPS	
# 4	Vapour barrier ②		Bitumen membrane	
# 3	12 mm CFB* ①	NA ①	80 mm EPS ①	①
# 2	0.75 mm trapeziodal steel deck			
# 1	Metal support structure			
Wind load	Low (1 m/s - 3 m/s)		Moderate (5 m/s - 8 m/s)	

*Table 2 - Material properties of the EPS, Glass-fleece, PVC membrane and bitumen used in the four tests. *Obtained from measurements in Netzsch HFM 446. Values without reference were taken from [7]*

Material	Parameter	Value
EPS	Density [kg/m^3]	25
	Thermal conductivity [W/(mK)]	0.034 – 0.035
Glass-Fleece	Density [kg/m^3]	100
	Area mass [kg/m^2]	0.12
	Specific heat capacity [J/(gK)]	1.7 - 2-0 [5]
Cement-bonded particle board (CPB)	Density [kg/m^3]	1350 – 1500
	Area density [kg/m^2]	16.2 – 18
	Thermal conductivity [W/(mK)]	0.200 – 0.287*
	Specific heat capacity [J/(gK)]	1.292 – 1.445*
PVC membrane	Heat of combustion [MJ/kg]	16.4 [6]
	Area density [kg/m^2]	2.1
Bitumen membrane	Heat of combustion [MJ/kg]	40.9 [7]

1.3. PV Array

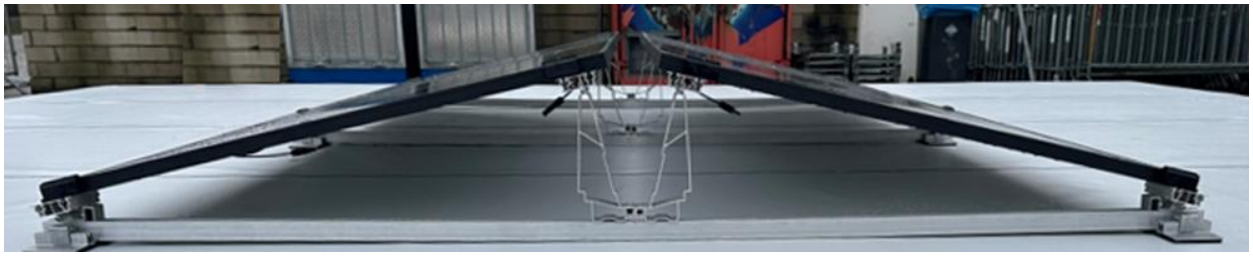

Figure 4 – Side view of the East/West-orientated PV array.

The PV array consisted of four Lynus monocrystalline photovoltaic (PV) modules with plastic-based back sheets. The array was mounted directly on the roofing membrane using an aluminium mounting system, without the use of ballast or mechanical fastening to the underlying roof construction. A side view of the building-applied photovoltaic (BAPV) mounting system is presented in Figure 4, which illustrates the 13° inclination of the PV modules, typical for East/West-oriented installations, and emphasizes the cross-section of the aluminium mounting components.

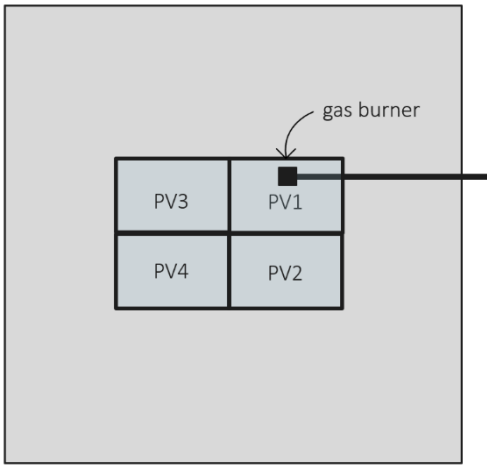

Figure 5 - Schematic of the PV array on the roof construction with corresponding numbering in accordance with their proximity to the gas burner. Not to scale.

1.4. Ignition source

A gas burner with a heat release rate (HRR) of 15 kW (± 1 kW), following the specifications presented in technical report CLC/TR 50670:2016 [10], was used as ignition source during the initial 10 minutes of the each test. The HRR was based on a of 324 mg/s (±20 mg/s) propane (95%) flow, monitored by a Bronkhorst flowmeter.

In all tests, the square-shaped gas burner was positioned at the midpoint along the width of the PV module consistently referred to as PV1, as illustrated in Figure 5. The horizontal distance from the burner's nearest edge to the lower edge of the PV module was 120 mm, while the vertical clearance between the bottom of the burner and the roof construction measured 80 mm.

1.5. Instrumentation

During the assembly of each roof build-up, a total of 27 thermocouples (TCs) were installed between the different layers in the construction. The TCs were sorted into three TC groups, where TCs in the same TC group were installed between the same layers in accordance with Table 1 where it is seen the TC group 3, with 14 TCs, located closest to the roof surface whereas TC group 1 is located on top of the steel deck.

- TC group 1: TC1-TC5
- TC group 2: TC6-TC12
- TC group 3: TC13-TC27

The number of thermocouples within each of the three TC groups of the varied depending on the proximity of the TC group to the top surface of the roof construction: a larger number of thermocouples were installed across TC group 3, always placed closest to the roof surface in order to quantify the temperature of the roof surface in case of flame spread. TC groups 1 and 2, positioned deeper in the construction instead consisted of a lower number of measurement points, mostly grouped in correspondence with the area beneath the PV array as depicted in Figure 6. Here the placement of the gas burner is shown in black with dotted lines in and the TCs have been colour coded depending on their proximity to the gas burner. These differentiations will be used in the temperature development plots in subsection 2.2.

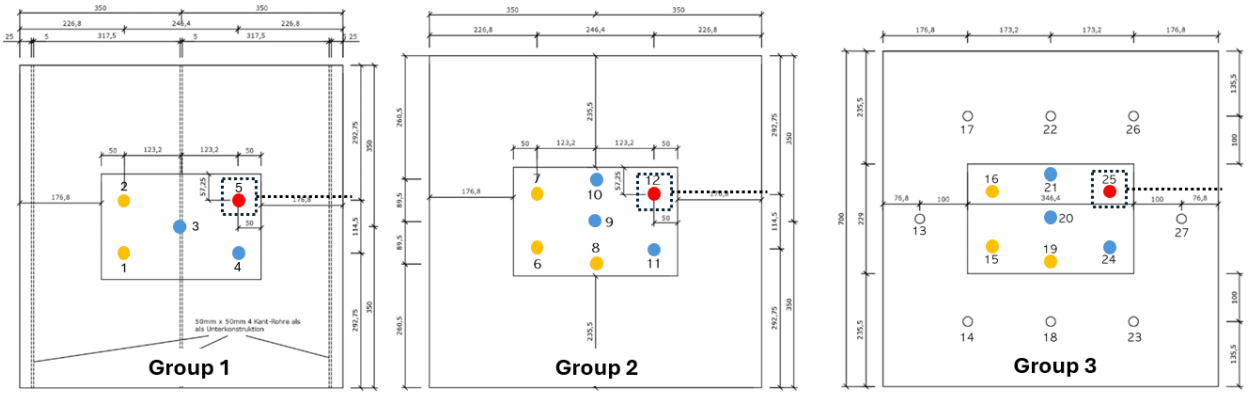

Figure 6 – Thermocouple distribution across the three different measurement layers.

2. TEST RESULTS

Visual observations illustrates that the outcome of the four tests, in the form of flame spread across the roof surface and heat transfer to the subjacent roof construction, relied on three factors. These are i) the type of roofing membrane (layer 7), ii) the material properties of the mitigation layer between the roofing membrane and underlying insulation material (layer 6) and iii) the ambient conditions, especially wind load, during the tests. The visual observations are discussed in the following subsections, which is followed by subsection 2.2 where relevant data from the thermocouples are presented to quantify the damage of the roof construction build-ups and to support, or explain, the visual observations.

2.1. Visual observations

Visual observations of flame spread along, and heat transfer into, the roof construction build-ups are analysed separately in the following two subsections. The analysis consists of visual observations and discussions of the factors that affected the outcome of the specific tests as well as differentiated the outcome across different tests.

2.1.1. Flame spread

Two flame spread trends were observed across the four tests, with test 2 representing an outlier from the consistent flame spread scenario seen in the remaining tests. In test 2, no self-sustained flame spread occurred outside the domain of the gas burner, whereas in the other three tests, the fire propagated within the cavity beneath all four PV modules. In these tests, no significant self-sustained flame spread was observed beyond the PV array, consistent with findings from previous large-scale tests [11], [12], [13].

In all four tests, the roofing membrane near the gas burner ignited within the first minutes after test initiation, as seen in the video frames from test 1 in Figure 7.1 to 7.2. Subsequently, radiative feedback, caused by flame deflection beneath PV1, heated the surrounding roof surface, leading to the release of combustible pyrolysis gases near the flame front [9], [14]. When the concentration of these gases exceeded their lower flammability limit, an additional area of the roof surface beneath PV1 ignited.

Focusing initially on three of the four tests (tests 1, 3, and 4), self-sustained flame spread continued within the cavity between the roof surface and the four PV modules, as illustrated by eight video frames from each test in Figure 7 to Figure 9. This behaviour was also observed in previous large-scale tests of BAPV systems on flat roof construction build-ups. [11], [12], [13].

After ignition of the roof surface near the gas burner below PV1, the larger area of ignited roofing membrane lead to an increased heat release rate and thus, further extension of the flames deflected below PV1 as described in medium scale experiments by Kristensen, Jacobs and Jomaas [9]. As a result, all the roofing membrane below PV1 ignited as seen in Figure 7 to Figure 9 subfigure 3.

As the extended flame below PV1 reached the gap between PV1 and PV2 (se*e Figure 5*), the combustion process occurred respectively within and outside the cavity between the roof surface and PV modules. The visible vertical flame between the two PV modules in Figure 7 to Figure 9 subfigures 3-4 represents the combustion process outside the cavity, whereas the one inside the cavity preheats the roofing membrane below PV2. The later leads to ignition below PV2 and the combined increased heat release rate from the burning membrane below PV1 and PV2, leads to continued flame spread below PV2 and PV4 as seen in Figure 7 to Figure 9 subfigures 5-7.

In all three tests with self-sustained flame spread below all PV modules, the fire self-extinguished and no significant self-sustained flame spread was observed outside the PV array. Self-extinguishment of the fire can be ascribed to insufficient access to one of the three components in the fire triangle: oxygen, fuel, or heat [15].

During the tests, failure of the mounting systems' aluminium profiles is observed, resulting in the collapse of the PV array onto the roof, as shown in Figure 7 to Figure 9 subfigures 5-6: because of this, available oxygen for the continuation of the combustion process is significantly reduced and, in conjunction with potential limited fuel left for combustion, self-extinguishment of the fire occurred.

Based on previous large-scale tests of flame spread below BAPV arrays [11], [12], [13], no significant fire spread was expected outside the cavity between the PV modules and the roof construction. This was confirmed in all three tests with self-sustained flame spread in the cavity, where no flame spread was observed outside the longer sides of the array facing the camera, with the charred area opposite to the camera-facing side in test 1, being the only exception.

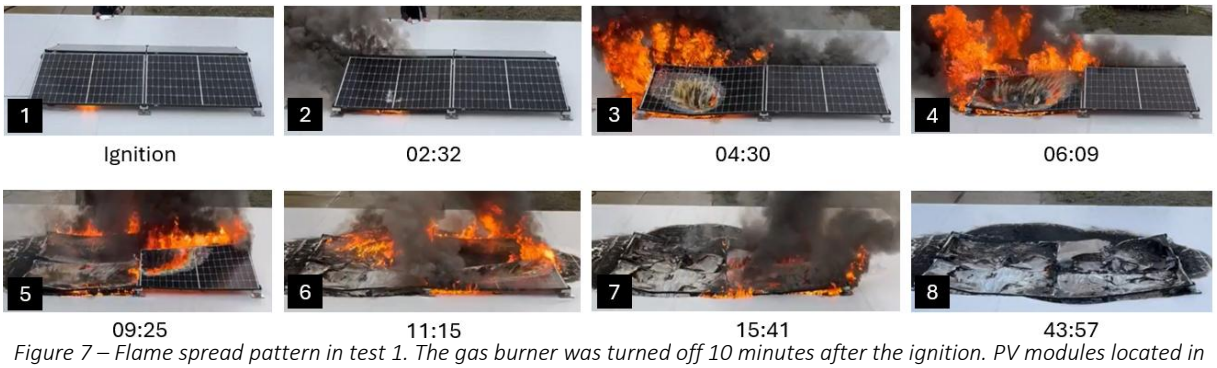

Figure 7 – Flame spread pattern in test 1. The gas burner was turned off 10 minutes after the ignition. PV modules located in accordance with Figure 5. Thus, PV1 is seen above the gas burner and the module on the right side of PV1 is PV3

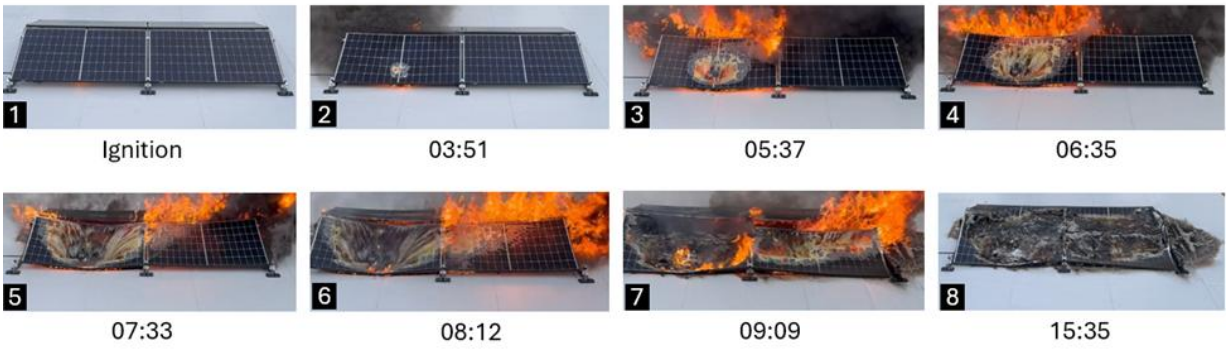

Figure 8 – Flame spread in test 3. PV modules located in accordance with Figure 5. Thus, PV1 is seen above the gas burner and PV3 is seen on the right side of PV1.

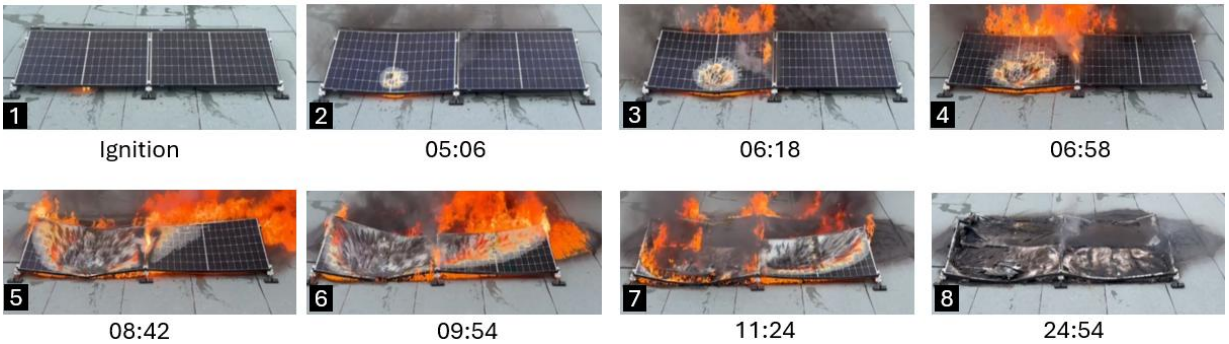

Figure 9 – Flame spread in test 4. PV modules located in accordance with Figure 5. Thus, PV1 is seen above the gas burner and the module on the right side of PV1 is PV3

However, the charred areas along the shorter sides of the three PV arrays in Figure 7 to Figure 9 subfigure 8 indicate that the surface of the roofing membrane ignited during the test, despite only a limited wind load being present during the four tests, particularly in tests 1 and 2, as illustrated by the near vertical smoke plume in Figure 10. In all three tests, the charred areas along the shorter edges of the arrays resulted from flames within the cavity deflecting towards the roof surface. This deflection facilitated the temporary ignition of the membrane seen in Figure 11, as the increased radiation from the deflected flames briefly raised the concentration of combustible gases above their lower flammability limit.

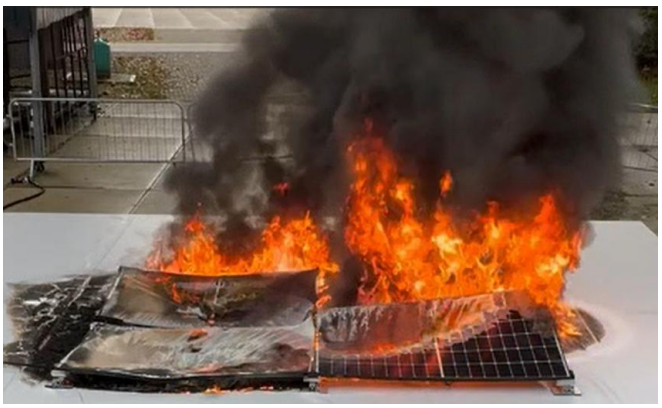

Figure 10 – Video frame from 10 minutes after ignition of test 1 illustrating the near vertical smoke plume caused by limited wind load.

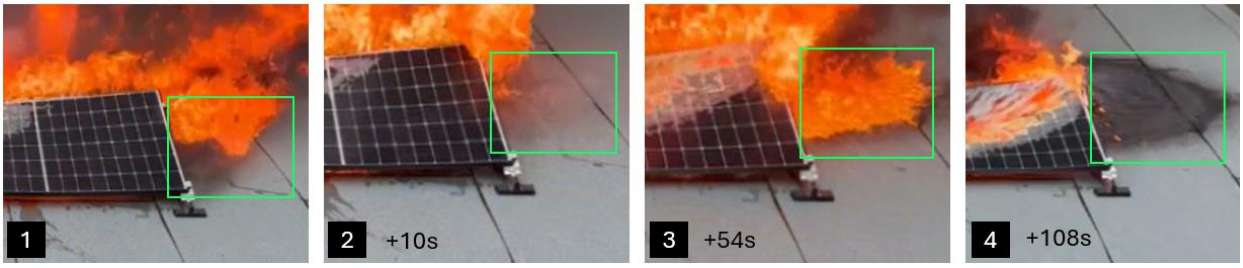

Figure 11 – Temporary ignition of the bitumen surface along the shorter side of the PV array in Test 4.

Without the radiative contribution from the deflected flames, the fire was extinguished as expected for a B_{ROOF}(t1)-compliant single-ply PVC membrane or Bitumen roofing on an open roof surface. As the wind direction was shifting, with the wind load in tests 3-4 being higher than in tests 1-2, it is expected that the wind caused deflection of the flames along edges of the PV arrays resulting in temporary ignition of the roof surface.

When comparing the flame spread process in tests 3 and 4 (Figure 8 and Figure 9), the overall trends in Subfigures 1–6 are similar. The slightly delayed flame spread in test 4, which was conducted with Bitumen rather than single-ply PVC, cannot be considered significant without test repetition. However, the overall test duration and combustion within the cavity were longer in test 4 due to the increased fuel load ascribed to the larger membrane thickness[1], and thus fuel load, of the Bitumen.

[1] Assumed to be 8 mm. Information based on manufacturer datasheet, since official test reports from Kiwa for Tests 3 and 4 were not available at the time this report was written.

In test 2, which was an outlier compared to the other tests and similar large-scale experiments [11], [12], [13], flame spread was confined to the area beneath PV1, as shown in Figure 12. Like tests 1 and 3, the PVC membrane near the gas burner ignited, but no self-sustained flame spread occurred during the ignition phase of the tests. Since flame spread occurred along the same PVC membrane in tests 1 and 3, the varying input parameters across the three tests are examined to understand why the flame spread was significantly less severe in test 2.

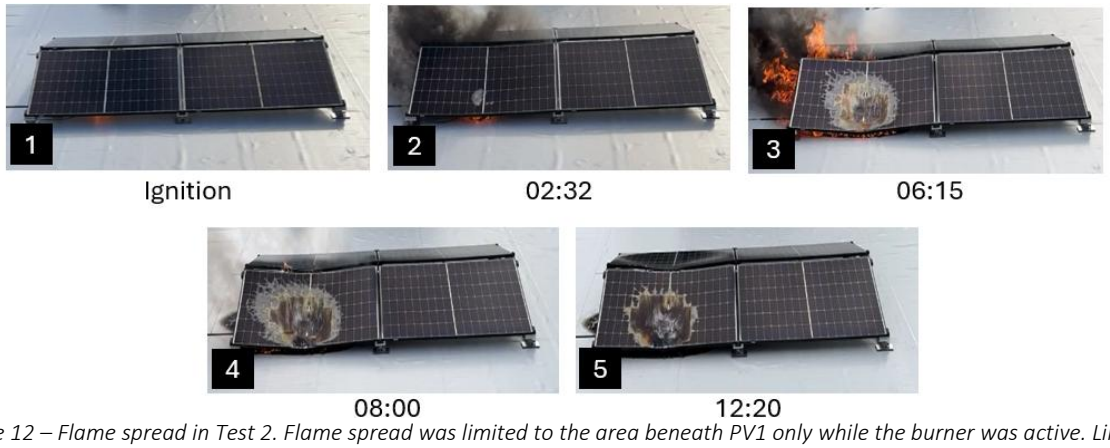

Figure 12 – Flame spread in Test 2. Flame spread was limited to the area beneath PV1 only while the burner was active. Limited damage to the PV array and remaining roof area was observed. PV modules located in accordance with Figure 5. PV1 is seen above the gas burner.

Two key parameters differed between the three tests: i) the mitigation layer of respectively 1.2 mm glass-fleece (test 1) and a 12 mm thick cement fibre board (tests 2-3), and ii) the wind load which was lower in tests 1-2 than tests 3-4. With the different flame spread patterns between tests 1 and 2 being caused by ignition of the EPS insulation in test 1, which will be further discussed in section 2.1.2, the influence of the different wind loads between tests 2 and 3 stands out as potential key differentiator between “flame spread” and “no flame spread”. However, the material properties of the CPB cannot be disregarded as the different consequences of tests 2 and 3 highlights the sensitivity of the fire dynamics in the cavity between the PV modules and roof surface, where even minor changes in ambient conditions, such as wind load or ambient temperature, can lead to significantly different outcomes.

Comparing the outcome of tests 2 and 3 with all publicly available large-scale tests conducted with PVC membranes [11], [12], [13], test 2 stands out as the sole test with no self-sustained spread flame, no matter the wind load in the other tests that where all conducted with a PVC membrane installed on either PIR insulation or mineral wool. Consequently, the wind load might not be a significant key parameter that generally differentiates “flame spread” from “no flame spread”, but it can a significant parameter if the overall energy balance of the fire dynamic system barely favours flame spread along the roofing membrane.

The different outcomes of tests 2 and 3 illustrates that the combined mass, specific heat capacity and conductivity of the CPB can act as a heat sink influencing the thermal equilibrium of the 1.8 mm thick PVC membrane, which can be assumed thermally thin. With flame spread being considered as a consecutive series of ignitions where ignition along the pre-heating zone only occurs when the material ahead of the flame front exceeds its ignition temperature, even small variables can render the difference between continuous flame spread and self-extinguishment. The thermal properties of cement-bonded particle board and potential role as a heat sink will be further discussed in section 2.1.2.

Based on the thermocouple data, it is known that the initial temperature of the roof build-ups was 10 °C higher in test 2 than in test 3. As such, less energy was required to elevate the temperature of the PVC membrane to its ignition temperature in test 2 and consequently, the heat transfer towards the pre-heating zone must have been higher in test 3 than in test 2.

As radiation from the 15 kW gas burner was the only significant heat transfer mechanism towards the roof surface during the initial phase of the tests, the view factor between the flame front and the roof surface defined the radiative heat transfer towards the roof surface [16]. Consequently, the higher wind load in test 3 likely resulted in a more concurrent flame spread scenario compared to the semi-concurrent flame spread scenario caused by flame deflection beneath the PV modules in all tests. As such, it is concluded that the boundary between “flame spread” and “no flame spread” relies on variable miniscule factors, which aligns with the identification of the critical gap height in medium-scale experiments [9].

To conclude, three of the four conducted tests replicate the outcome from previous large-scale tests, whereas test 2 represented an outlier not seen in other public accessible large-scale tests of BAPV modules on flat roof construction build-ups. As the outcome of test 2 was not replicated in test 3, the reduced flame spread cannot solely be ascribed to the CPB acting as a heat sink, nor to the reduced wind load, but to an insufficient overall energy balance within the fire dynamic system.

2.1.2. Damage of roof construction below the roofing membrane

In the tests, two distinct trends were observed regarding the propagation of the fire into the deeper layers of the roof construction build-ups. These are i) ignition of, and flame spread into, the EPS insulation, and ii) no ignition and limited melting of the EPS insulation.

Figure 13 – From the end of test 1, where the EPS was initially ignited and subsequently melted below the PV array. The closest PV modules are PV4 (left) and PV2 (right) in accordance with Figure 5.

Figure 14 – From test 1. Yellow line indicates the original edge of the PV modules PV 4 and PV 3. The dotted red line marks the edge of melted EPS. Cutting of single-ply PVC membrane done by KIWA for the test report during inspection of roof damage.

As mentioned in Section 2.1.1, the EPS was ignited in test 1 and all the EPS melted below the PV system as indicated from the level of the collapsed PV array in Figure 13. It is expected that ignition of the EPS occurred as the result of either mechanical or thermal failure of the double layered 1.2 mm thick glass-fleece installed between the surface of EPS and PVC membrane. After the initial ignition of the EPS, the adjacent EPS melted and retracted, which prevented selfsustained flame spread within the insulation material. Consequently, no water was used for extinguishment.

In line with the horizontal flame spread pattern, the affected part of the roof construction was confined by the footprint of the BAPV array and as such, melted EPS was solely observed near the perimeter of the BAPV array as illustrated in Figure 14.

During KIWAs following examination of the roof built up below the BAPV array in test 1, the vapour barrier installed below the EPS insulation was found to be intact at the location examined, as illustrated in Figure 15. The intact vapour barrier indicates retraction of the EPS which at the examined location prevented self-sustained flame spread within the EPS. The remaining part of the roof was not examined on the test day, but afterwards the employees at Twente Safety Centre disassembled the roof build-up. No damage was observed at the trapezoidal steel deck as showed in Figure 16.

Compared to the outcome of test 1, the thermal exposure and physical damage of the insulation material was significantly less severe in the remaining tests which were conducted with the cement fibre board (CPB) as a mitigation layer on top of the EPS. In tests 2 and 3, with the roofing membrane being a single-ply PVC membrane, a local cavity within the EPS was formed at the location of the gas burner used for ignition.

In both tests, the depth of the cavity was no more than 10 cm with a diameter lower than 20 cm as seen from the images in Figure 17. In both tests, gas burner was located above assemblies of the CPBs. In the final test, test 4 conducted with 8 mm of Bitumen membrane, no melted EPS was observed below the mitigation layer.

The combined observations from the in-depth damage patterns in the three tests, combined with the location of the gas burner, indicates that the

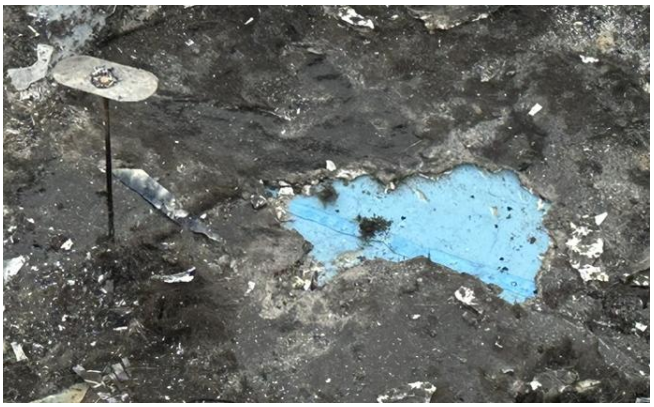

Figure 15 – From test 1. Intact vapour barrier observed below melted and charred EPS at the examined location.

Figure 16 – From test 1. Trapezoidal steel deck after disassembly of the roof build-up. No residue from droplets formed by melted EPS noticed by the team at Troned test facility. From KIWA report.

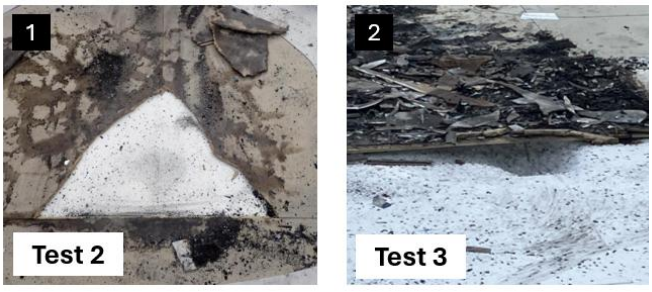

Figure 17 – Melted EPS insulation below the cement-bonded particle board. Notice that cavities were located below intersections between three (left) and two (right) boards.

heat transfer from the burning roofing membranes towards the EPS insulation was insignificant in the two tests with self-sustained flame spread (tests 3 and 4), since the damage within the EPS insulation was similar in the tests with and without self-sustained flame spread (test 2 and 3).

As such, the tests indicated that the cavities within the EPS, caused by a local temperature increase, in tests 2 and 3 was the result of heat transfer from the gas burner during the ignition phase, rather than from the combustion process in the cavity between the roof surface and PV array.

In the post-test examination of test 4, it was observed that only the upper layer of the two-layer Bitumen membrane was significantly damaged during the fire below the BAPV array, whereas the lower layer had not been part of the combustion process, which can be explained by one of, or a combination of two things limiting the duration of the combustion process:

- Reduced fuel availability, as inert components of the upper Bitumen layer become predominant with the reduction of combustible fuels caused be combustion.
- Reduced oxygen availability due to the collapse of the PV arrays mounting system as discussed in subsection 2.1.1.

To conclude, visual observations of the roof build-ups in four tests conducted, indicates that the thermal properties of the cement fiber board installed above the EPS in tests 2, 3 and 4 have the potential to mitigate the consequences of a PV-related fire significantly. The reason for that is, that the material serves as a heat sink. A $1\ ℃$ temperature increase of the cement-bonded particle board would require net heat transfer of $21\ kJ/m^2$ ($c_p = 1.3\ kJ/kg\,K$ and $\rho = 1350\ kg/m^3$), but the local temperature increase would be temporary as the energy is transferred within the CPB to maintain an overall energy equilibrium. Because of the CPBs higher conductivity, the internal energy transfer occurs 6-8 times faster than within insulations products such as EPS or mineral wool due to its higher conductivity of 0.200-0.287 W/(mK) in accordance with Table 2.

In short: the cement-bonded particle board acts as a heat sink that requires i) more energy to heat up, and ii) distributes the energy faster than insulation products which ultimately distributes energy away from the pyrolysis and pre-heating zone.

2.2. Thermocouple measurements during the tests

Thermocouples (TCs) were installed between the different layers of the roof constructions to evaluate the effect of the heat transfer from the fire during each test and to validate the visual observations presented in Section 2.1.The installation of the TC groups within the different layers of the constructions follows the positioning in accordance with the red crosses previously presented in Table 1 and Figure 6.

While in tests 2-4 two different TC groups were placed above and below the mitigation layer (TC Group 3 and 2 respectively), test 1 was characterized by the presence of an individual TC Group positioned beneath the glass-fleece layer only. Figure 18 shows the temperature development for TC Group 3 of test 1. An understanding of both flame spread across and into, the roof construction for test 1 can be inferred from these measurements.

Due to its proximity to the burner and placement corresponding to the ignition location, TC25 is the first TC to record a significant temperature increase due to heat transfer from the gas burner and radiative re-radiation from the deflected flame below PV1 (see Figure 5) onto the roof construction.

Thereafter, the flame spread across the roof can be understood by looking at the different onset times of the remaining thermocouples and by observing 1st peak in the temperature curves of Figure 18 and Figure 19. After ignition of the PVC membrane beneath PV1, the fire spreads to the cavity below PV2 and the temperature measured by TC24 increases consequently, which corresponds to the flame spread pattern in Figure 7.1-2. Transition to the adjacent areas of the roof follows as intermediate TC19-21 placed in the middle of the array between PV1-PV2 and PV3-PV4 start increasing simultaneously. Finally, once the flame spread reaches PV3 and PV4, the temperatures of TC15 and TC16 increase.

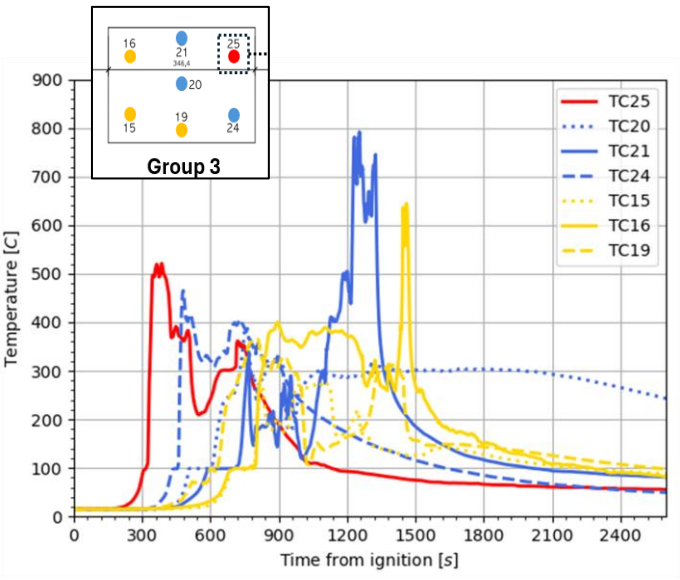

Figure 18 – Temperature development measured in between the glass-fleece and EPS insulation measured by TC group 3 in test 1. Location of the individual TCs marked in the upper left corner in correspondence with Figure 6.

Contrary to test 1, tests 2, 3 and 4 share the same TC Group placements within the construction layers, allowing a more straightforward comparison between the temperature measurements. Above all, differentiation in the flame spread across and into the roof can be made more distinctively. Namely TC Group 3, placed between the roof membrane and the cement-bonded particle board, can be utilized for the analysis of the fire spread; TC Group 2 positioned below the cement-bonded particle board highlights the heat transfer into the subjacent roof construction. Similarly to what was seen in Figure 18 for test 1, the thermocouples positioned as TC25 were the first to record a temperature increase in tests 2-4 due to its immediacy with the ignition source, as seen in Figure 19.

As flame spread only occurred along the area below PV1 in test 2, it is reflected by the temperature measurements, where only TC25 and the adjacent TC20 and TC21 monitor significant temperature increases. On the contrary, all thermocouples installed in the layer closest to the roof surface, TC Group 3, measure significant temperature increases, which corresponds to the flame spread patterns seen in Figure 8 and Figure 9. The increased flame spread rate, most likely facilitated by the slightly higher wind load, can be observed by the shorter thermocouple activation times compared to those from tests 1 and 2. Similarly to test 1, similar flame spread dynamics across the roof are seen in test 3 and test 4 where TC24 activates as the fire spreads below PV2, followed by the TCs placed in the middle of the roof and ending with the thermocouples placed below PV3 and PV4.

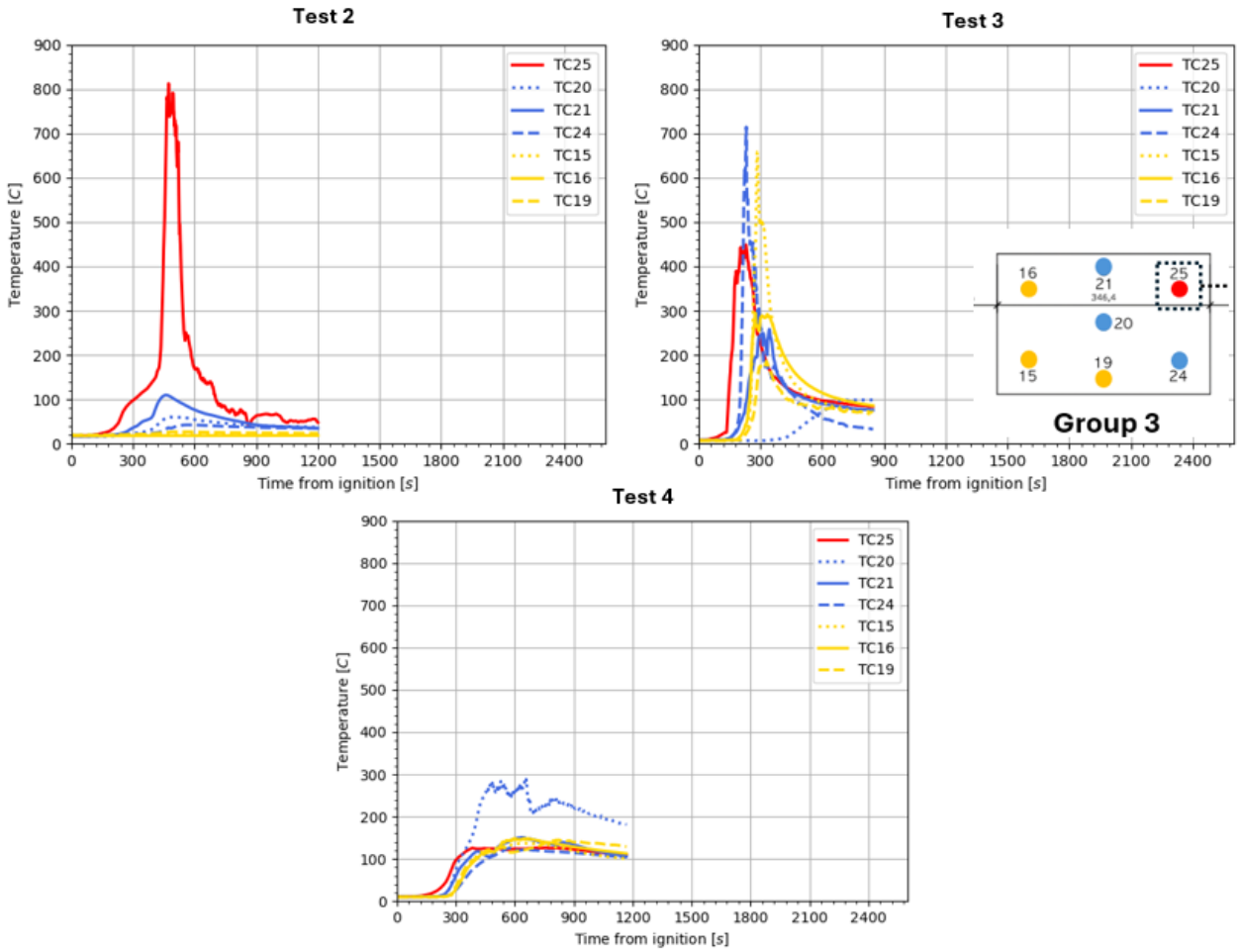

Figure 19 – Temperature development measured by thermocouples (TC) installed below roofing membrane (TC Group 3) in tests 2,3 and 4. Location of the individual TCs outlined in lower right side of the plot for test 3 (upper right), in correspondence with Figure 6.

When comparing tests 2 and 3 to test 4, more pronounced temperature dynamics are observed in the former, including rapid temperature rise, a higher peak temperature in the test involving self-sustained flame spread beneath the PV array (test 3), and a faster post-peak temperature decay. This behavior contrasts markedly with the slower temperature development and near-steady-state condition observed in test 4. The pronounced differences are ascribed to the material parameters of respectively the 1.8 mm thick PVC membrane in tests 2-3 and the 8 mm thick dual-layer Bitumen-based membrane examined in test 4.

The reason for that is that the limited thickness of the PVC membrane can be assumed to be near thermally thin, whereas the 8 mm thick Bitumen membrane is considered thermally thick. Thus, a near uniform temperature distribution is expected across the thickness of the PVC membrane, whereas significant temperature difference is expected between upper and lower side of the 8 mm thick Bitumen. Consequently, the lower section of the Bitumen serves as an additional layer of insulation between the pyrolysis zone and the subjacent cement-bonded particle board.

Since the fire in the cavity self-extinguished in both tests 3 and 4, as discussed in section 2.1, either due to lack of fuel or oxygen, the temperature either declines or remains relatively constant depending on the boundary conditions surrounding the thermocouples.

In test 4, the significantly elevated steady-state temperature recorded by TC20 (see Figure 19) constitutes an outlier. This anomaly may be attributed to intensified radiative heating at the center of the PV array, potentially followed by upward penetration of the thermocouple through the bitumen membrane, facilitated by an increased thermal degradation of the membrane material.

The temperature data from TC Group 2, placed below the cement-bonded particle board, shows how the heat transfer from the surface area, involved in the fire, transitions into the deeper layers of the roof construction build-ups as plotted in Figure 20.

The temperature data from TC Group 2, placed below the cement-bonded particle board, shows how the heat from the roof area involved in the fire transitions into the deeper layers of the construction. In test 2, since the fire spread was limited to PV1, only TC12 installed subjacent to the heated area was affected, measuring a maximum temperature of 95°C. For tests 3 and 4 instead, all TCs in Group 2 increase as the fire propagates along the roof surface below the BAPV array. In those tests, maximum temperatures of 100°C were reached and maintained until the end of the test. These temperature measurements may be the result of water vapour

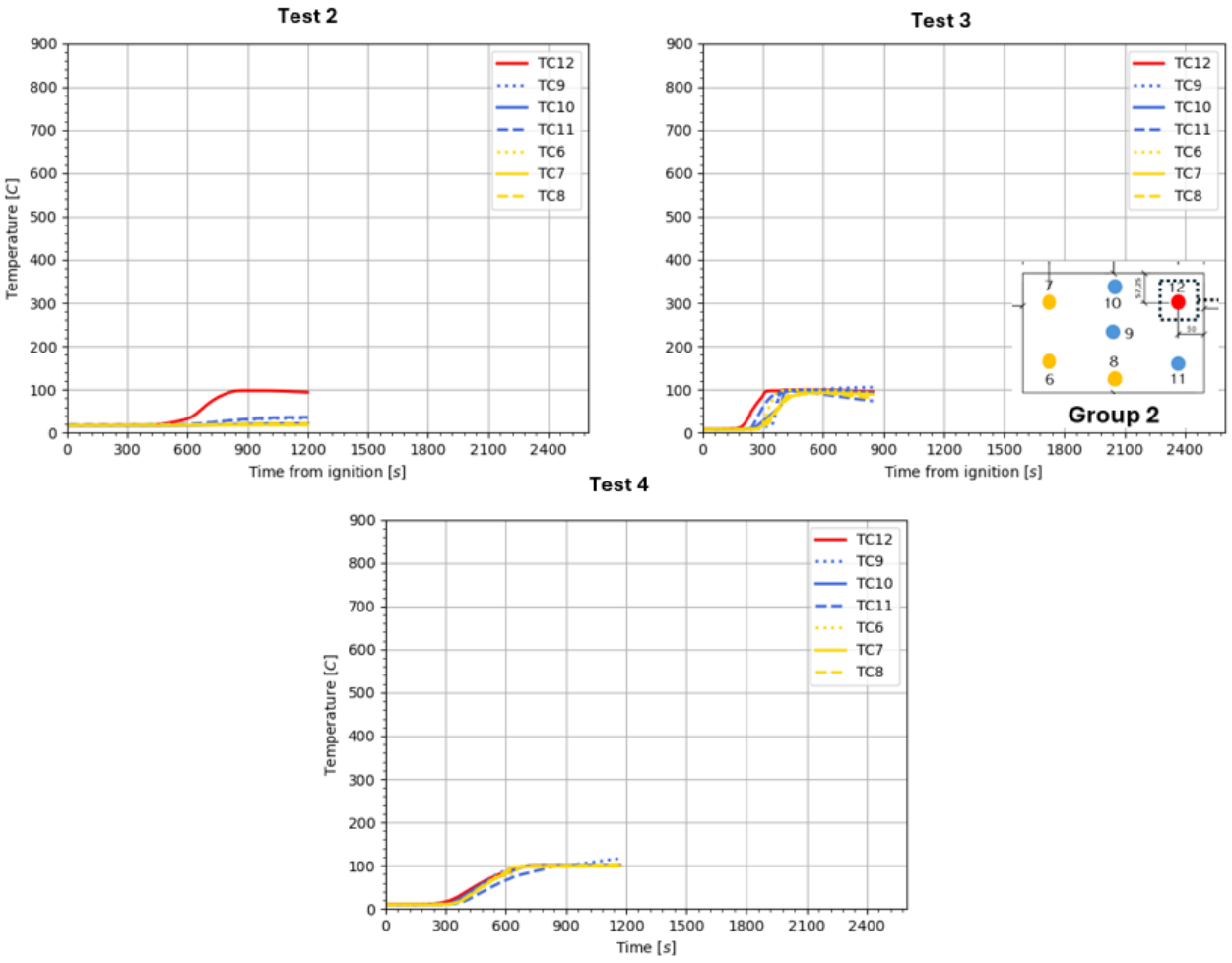

Figure 20 – Temperature development measured by thermocouples (TC) installed below cement-bonded particle board and EPS insulation (TC Group 2) in Tests 2,3 and 4. Location of the individual TCs outlined in lower right side of the plot for test 3 (upper right), in correspondence with Figure 6.

released from the cement particleboard caused by the heating process from the fire, especially since cement-bonded particle board is characterized by an inherent stored water content around 10 % [17].

If the temperature increase to maximum 100°C was not caused by the release of water vapor, but conductive heat transfer through the cement-bonded particle board, it is expected that the different initial ambient temperatures of around 20 °C, 10 °C and 10 °C in respectively tests 2, 3, and 4 (see Figure 20), combined with the different fuel load ascribed to the roofing membranes would render significantly different temperature development across the three tests.

Finally, it should be noted that no significant temperature development was measured in TC1-TC5 installed on top of the 0.75 mm thick trapezoidal steel beck, nor TC13-TC14, TC17-TC18, TC22-TC23 and TC26-TC27 installed outside the PV array as illustrated in Figure 6. As no visual damage was observed on the steel deck or outside the PV array at the location of the Thermocouples, the temperature measurements are not plotted.

3. CONCLUSION

A series of four large-scale fire tests designed by IVH, the German Rigid Foam Industry Association and EUMEPS, the European Manufacturers of Expanded Polystyrene were conducted to examine the impact of PV-related fires in the cavity between an east/west orientated BAPV array with four modules and four different roof construction built-ups. A total of three parameters, being i) the roofing membrane, ii) the material layer between the EPS insulation containing a polymeric fire retardant (Class E reaction to fire) and the roofing membrane, and iii) the ambient conditions, were varied across the tests to access methods to mitigate the consequences of a PV related fire.

In tests 1-3 a 1.8 mm thick Bauder Thermofol M18 (B_{ROOF}(t1)) PVC membrane was used as roof covering, whereas an 8 mm thick two-layer Bitumen-based roof covering (B_{ROOF}(t1)) was examined in test 4. 1.2 mm glass-fleece was installed between the PVC membrane and EPS insulation in test 1, whereas a 12 mm thick cement-bonded particle board was installed between the EPS and roof covering in tests 2-4. Based on the four tests, the following conclusions can be drawn:

- The fire propagated along the roof surface below the PV array in all tests except test 2 where the fire did not propagate outside the domain of the ignition source.
- In test 1, the fire below the PV modules penetrated the 1.2 mm thick glass-fleece between the PVC membrane and EPS insulation. The EPS was ignited, but no self-sustained flame spread occurred outside the footprint of the PV array.
- In tests 3 and 4, the cement-bonded particle board (CPB) protected the subjacent layer of EPS. As such, no damage of the EPS was observed below the CPB, except the formation of a small cavity below the location of the ignition source in test 3.
- A similar cavity with a maximum diameter and depth of respectively 20 cm and 10 cm was observed below the location of the ignition source in test 2. Thus, it is concluded that the voids of melted EPS in tests 3 was caused by heat transfer from the ignition source and not the fire propagating above the CFB.
- Based on the results from the four tests, it can be concluded that the consequences of a PV-related fire can be mitigated if a correctly installed thermal barrier with appropriate properties, such as the 12 mm thick cement-bonded particle board, is introduced between the roofing membrane and the underlying

EPS insulation. It should be considered to use 2x6 mm thick cement-bonded particle board with staggered joints.

REFERENCES

[1] International Energy Agency (IEA), "Integrating Solar and Wind."
[2] Swiss RE Insititute, "Rooftop solar: Emerging risk control needs for properties." Accessed: Oct. 03, 2024. [Online]. Available: https://www.swissre.com/institute/research/topics-and-risk-dialogues/climate-and-natural-catastrophe-risk/emerging-risk-control-needs-for-properties.html
[3] R. Stølen, J. S. Fjærestad, and R. F. Mikalsen, *EBOB – Solcelleinstallasjonar på bygg, Del 2: Teknisk rapport. Eksperimentell studie av brannspreiing i holrom bak solcellemodular på skrå takflater.* 2022. Accessed: Sept. 30, 2022. [Online]. Available: https://risefr.com/media/rapporter/rise-rapport-2022-83-solcelleinstallasjoner-pa-bygg-teknisk-rapport.pdf
[4] J. S. Kristensen, "Fire risk associated with photovoltaic installations on flat roof constructions - Experimental analysis of fire spread in semi-enclosures," Doctor of Philosophy, The University of Edinburgh, Edinburgh, 2022. Accessed: July 25, 2023. [Online]. Available: http://dx.doi.org/10.7488/era/3170
[5] Ulrich Meier, "Large-scale fire test on a flat roof system with EPS insulation and a glass-fleece fire barrier," Kiwa BDA Testing, Test report 24L0474/2 REV 02, Feb. 2025.
[6] Ulrich Meier, "Large-scale fire test on a flat roof system with EPS insulation and a cement-bonded particle board fire barrier," Test report 24L0474/3 REV 02, Feb. 2025.
[7] Ulrich Meier, "Large-scale fire test on a flat roof system with EPS insulation and a cement-bonded particle board fire barrier, with a PVC roof waterproofing sheet," Test report 25L0053/1, Apr. 2025.
[8] Ulrich Meier, "Large-scale fire test on a flat roof system with EPS insulation and a cement-bonded particle board fire barrier, with a bitumen roof waterproofing sheet," Test report 25L0053/2, Apr. 2025.
[9] J. S. Kristensen, B. Jacobs, and G. Jomaas, "Experimental Study of the Fire Dynamics in a Semi-enclosure Formed by Photovoltaic (PV) Installations on Flat Roof Constructions," *Fire Technol.*, 2022, doi: 10.1007/s10694-022-01228-z.
[10] CLC/TR 50670, "External fire exposure to roofs in combination with photovoltaic (PV) arrays – Test method(s)," 2016.
[11] J. S. Kristensen and G. Jomaas, "Experimental Study of the Fire Behaviour on Flat Roof Constructions with Multiple Photovoltaic (PV) Panels," *Fire Technol.*, vol. 54, no. 6, pp. 1807–1828, 2018, doi: 10.1007/s10694-018-0772-5.
[12] PU Europe, "PU Europe Factsheet #24 Fire performance of thermal insulation products in end-use conditions." PU Europe, June 2022. Accessed: July 24, 2023. [Online]. Available: https://www.pu-europe.eu/factsheet-24e-test-report-now-available/
[13] KINGSPAN, "The Performance of Two Dutch Flat Roof Constructions in the Event of a Fire in a PV System - A White Paper." Kingspan Insulation B.V., Jan. 2025. Accessed: Mar. 13, 2025. [Online]. Available: https://www.kingspan.com/content/dam/kingspan/kil/campaigns/kice/kingspan-pv-on-flat-roof-fire-testing-white-paper-en-nl-v2.pdf
[14] X. Ju *et al.*, "Correlation analysis of heat flux and fire behaviour and hazards of polycrystalline silicon photovoltaic panels," *IOP Conf Ser Mater Sci Eng*, vol. 201, no. 1, 2017, doi: 10.1088/1757-899X/201/1/012036.
[15] B. Merci and T. Beji, *Fluid mechanics aspects of fire and smoke dynamics in enclosures*. 2016. doi: 10.1201/b21320.
[16] J. G. Quintiere, "Fire Spread on Surfaces and Through Solid Media," in *Fundamentals of Fire Phenomena*, John Wiley & Sons, Ltd, 2006.
[17] A. R. Hameete, "Large-scale fire test on a flat roof system with EPS insulation and a cement-bonded particle board fire barrier," Kiwa BDA Testing, 24L0474/3, Feb. 2025.